Available online at www.sciencedirect.com
ScienceDirect
Journal of Sound and Vibration 322 (2009) 8–14
JOURNAL OF SOUND AND VIBRATION
www.elsevier.com/locate/jsvi

Rapid Communication

# Asymmetric solutions in large amplitude free periodic vibrations of plates

Pedro Ribeiro*

*DEMEGI/IDMEC, Faculdade de Engenharia, Universidade de Porto, R. Dr. Roberto Frias, s/n, 4200-465 Porto, Portugal*

Received 27 October 2008; received in revised form 31 December 2008; accepted 12 January 2009
Handling Editor: M.P. Cartmell
Available online 20 February 2009

**Abstract**

When the in-plane inertia is neglected, the equations of motion that represent free, large amplitude, periodic vibrations of perfect plates only contain cubic nonlinear terms. It is here shown that, unlike often assumed, these equations admit asymmetric solutions. For that purpose, the time domain equations of motion are mapped into the frequency domain by the harmonic balance method, keeping the constant term and the second harmonic in the truncated Fourier expansion of the transverse displacements. A test plate is analysed and a bifurcation due to a 1:2 internal resonance is found. This bifurcation results in a branch of solutions where the equilibrium position is not the flat one and where odd and even harmonics coexist.


## 1. Introduction

Very often it is assumed that the transverse, periodic, large displacement, free vibrations of perfect (i.e., flat at rest) beams and plates occur about the flat equilibrium position and only involve odd harmonics (see for example Refs. [1–11]). One justification for this assumption is that, if one neglects the in-plane inertia and if the plate is perfect, the nonlinear equations of motion only contain cubic nonlinear terms. It is recalled and demonstrated in this rapid communication that bifurcations may occur, causing the appearance of asymmetric solutions, which contain a constant term and even harmonics. Even harmonics have been previously found in experimental analysis (Refs. [5,12]).

## 2. Formulation

The time domain ordinary differential equations of motion here employed to represent the geometrically nonlinear oscillations of perfect plates are the ones obtained in Ref. [1], therefore, only the essential steps are presented. A right-handed three-dimensional Cartesian coordinate system is adopted, with the $x$ and $y$ axis on the middle plane of the undeformed plate and the $z$ axis positive upwards. The origin of the coordinate system is located in the geometric centre of the undeformed plate. The middle plane displacement components in the

*Tel.: +351 22 508 17 16; fax: +351 22 508 14 45.
*E-mail address:* pmleal@fe.up.pt

0022-460X/$ - see front matter © 2009 Elsevier Ltd. All rights reserved.
doi:10.1016/j.jsv.2009.01.037

$x$, $y$ and $z$ directions are represented by $u_0$, $v_0$, $w_0$, respectively, and are expressed in the form:

$$\begin{Bmatrix} u_0(x,y,t) \\ v_0(x,y,t) \\ w_0(x,y,t) \end{Bmatrix} = \mathbf{N}(x,y) \begin{Bmatrix} \mathbf{q}_u(t) \\ \mathbf{q}_v(t) \\ \mathbf{q}_w(t) \end{Bmatrix} \tag{1}$$

where $\mathbf{N}(x, y)$ is the matrix of shape functions, which is formed by row vectors of shape functions associated with each displacement component as follows:

$$\mathbf{N}(x,y) = \begin{bmatrix} \mathbf{N}_u(x,y)^T & \mathbf{0} & \mathbf{0} \\ \mathbf{0} & \mathbf{N}_v(x,y)^T & \mathbf{0} \\ \mathbf{0} & \mathbf{0} & \mathbf{N}_w(x,y)^T \end{bmatrix} \tag{2}$$

The sets of shape functions used here are the sets of polynomials employed in Ref. [1]. Vectors $\mathbf{q}_i(t)$, $i = u, v, w$, which appear in Eq. (1), are vectors of generalized displacements constituted by three subsets ordered as follows: in-plane along the $x$ axis, in-plane along the $y$ axis, transverse along the $z$ axis.

The plates are assumed to be initially flat, i.e., without geometric imperfections [13,14], and Von Kármán's nonlinear strain–displacement relationships [14,15]

$$\begin{Bmatrix} \varepsilon_x \\ \varepsilon_y \\ \gamma_{xy} \end{Bmatrix} = \begin{Bmatrix} u_{,x} - w_{,xx} + \dfrac{zw_{,x}^2}{2} \\ v_{,y} - w_{,yy} + \dfrac{zw_{,y}^2}{2} \\ u_{,y} + v_{,x} - 2w_{,xy} + zw_{,x}w_{,y} \end{Bmatrix} \tag{3}$$

are adopted. In Eq. (3) $\varepsilon_x$ and $\varepsilon_y$ represent the strains in the $x$ and $y$ directions, and $\gamma_{xy}$ represents the engineering shear strain.

To analyse periodic vibrations of plates with fixed ends one can most often neglect the in-plane inertia [16] and a reduced system of equations of motion on $\mathbf{q}_w(t)$ is achieved. This system has the form:

$$\mathbf{M}\ddot{\mathbf{q}}_w(t) + \mathbf{K}_\ell \mathbf{q}_w(t) + \mathbf{K}_{n\ell}(\mathbf{q}_w(t))\mathbf{q}_w(t) = \mathbf{0} \tag{4}$$

All terms of the nonlinear stiffness matrix $\mathbf{K}_{n\ell}(\mathbf{q}_w(t))$ are quadratic functions of the generalized transverse displacements $\mathbf{q}_w(t)$, hence, Eq. (4) only contain cubic nonlinear terms. $\mathbf{M}$ represents the mass matrix and $\mathbf{K}_\ell$ the stiffness matrix of the linear structure, both constant.

To further reduce the number of equations of motion, a reduced set of $m$ modal coordinates is chosen:

$$\mathbf{q}_w(t) \cong \mathbf{\Phi}_{\mathrm{n}\times\mathrm{m}} \mathbf{q}_m(t) \tag{5}$$

and a condensed set of equations is derived from (4). Matrix $\mathbf{\Phi}_{n\times m}$ is a rectangular matrix with the selected subset of the modal eigenvectors. Modal reduction is a classic procedure in linear systems and has been explained in a context similar to the present one in Ref. [17]. The form of the system of equations in modal coordinates is similar to Eq. (4), as represented by

$$\mathbf{M}^m\ddot{\mathbf{q}}_m(t) + \mathbf{K}_\ell^m \mathbf{q}_m(t) + \mathbf{K}_{n\ell}^m(\mathbf{q}_m(t))\mathbf{q}_m(t) = \mathbf{0} \tag{6}$$

The superscript $^m$ in the matrices simply indicates that they result from modal reduction.

Steady-state, periodic solutions will be determined using the harmonic balance method to solve Eq. (6), hence, $\mathbf{q}_m(t)$ is written as a truncated Fourier series. To be able to detect oscillations that do not occur about the flat configuration, the constant term and at least one even harmonic should be considered. In addition, we know from Refs. [1,9] that internal resonances of type 1:3 occur in free, large displacement amplitude vibrations of plates. Vector $\mathbf{q}_m(t)$ will therefore be written as

$$\mathbf{q}_m(t) = \frac{1}{2}\mathbf{w}_0^m + \sum_{i=1}^{3} \mathbf{w}_i^m \cos(i\omega t) \tag{7}$$

Inserting expansion (7) into the equations of motion (4) and employing the harmonic balance method, an algebraic set of equations of motion of the form

$$\left(-\omega^2\begin{bmatrix}\mathbf{0}&\mathbf{0}&\mathbf{0}&\mathbf{0}\\ \mathbf{0}&\mathbf{M}^m&\mathbf{0}&\mathbf{0}\\ \mathbf{0}&\mathbf{0}&4\mathbf{M}^m&\mathbf{0}\\ \mathbf{0}&\mathbf{0}&\mathbf{0}&9\mathbf{M}^m\end{bmatrix}+\begin{bmatrix}\frac{1}{2}\mathbf{K}_\ell^m&\mathbf{0}&\mathbf{0}&\mathbf{0}\\ \mathbf{0}&\mathbf{K}_\ell^m&\mathbf{0}&\mathbf{0}\\ \mathbf{0}&\mathbf{0}&\mathbf{K}_\ell^m&\mathbf{0}\\ \mathbf{0}&\mathbf{0}&\mathbf{0}&\mathbf{K}_\ell^m\end{bmatrix}\right)\begin{Bmatrix}\mathbf{w}_0^m\\ \mathbf{w}_1^m\\ \mathbf{w}_2^m\\ \mathbf{w}_3^m\end{Bmatrix}+\begin{Bmatrix}\frac{1}{2}\mathbf{F}_0(\omega,\mathbf{w})\\ \mathbf{F}_1(\omega,\mathbf{w})\\ \mathbf{F}_2(\omega,\mathbf{w})\\ \mathbf{F}_3(\omega,\mathbf{w})\end{Bmatrix}=\begin{Bmatrix}\mathbf{0}\\ \mathbf{0}\\ \mathbf{0}\\ \mathbf{0}\end{Bmatrix} \tag{8}$$

is obtained. Vector $\mathbf{w}$ groups vectors $\mathbf{w}_i^m$, $i=0$–3. Each vector $\mathbf{F}_i(\omega,\mathbf{w})$ in the former equation is defined as

$$\mathbf{F}_i(\omega,\mathbf{w})=\frac{2}{T}\int_0^T \mathbf{K}_{n\ell}^m(\mathbf{q}_m(t))\mathbf{q}_m(t)\cos(i\omega t)\,\mathrm{d}t,\quad i=0,1,2,3 \tag{9}$$

with $T$ representing the period of vibration. The set of algebraic equations (8) will be solved by an arc-length continuation method, which has been used before (Refs. [1,7,18] for example) and details are not given here. The method is able to find more than one steady-state solution for a particular fundamental frequency of series (7). The initial conditions, which are not of interest in our analysis, would determine to which of the possible steady-state solutions, i.e., to which attractor, the system would converge. Refs. [1,7,18] can also be consulted to learn how secondary branches are detected and followed. In short: to switch the continuation into a secondary branch, the eigenvectors of the Jacobian matrix computed at the bifurcation point are used to define a predictor and this predictor is then corrected, until the frequency domain equations of motion are respected.

## 3. Demonstrative numerical example

The proof that asymmetric solutions with even harmonics appear in the geometrically nonlinear free vibration of initially perfect plates will be made by means of an example. The particular plate under analysis here is the rectangular, isotropic, thin and fully clamped plate with immovable boundaries analysed in Ref. [1]. The geometric properties of this plate are: $b/a=1.0667$ (length/width), $a/h=300$ (width/thickness), $h=0.001$ m. The material properties are typical of aluminium: $E=7\times10^{10}\,\mathrm{N/m^2}$ (Young's modulus), $\rho=2778\,\mathrm{kg/m^3}$ (mass density), $\nu=0.34$ (Poisson's ratio).

One hundred shape functions for the displacements in the $x$ direction, 100 for displacements in the $y$ direction, and forty nine for displacements in the $z$ direction are employed. Hence, the matrix of shape functions, Eq. (2), is a $249\times249$ matrix. Numerical tests indicate that the model with this number of shape functions provides a quite good approximation for the lower order modes of vibration. As explained before, modal reduction was implemented, and in this particular case the first 15 modes of vibration were used in Eq. (5), i.e. $m=15$. Again, numerical tests, including comparison with non-reduced models, indicated that this number of modes is enough to achieve good accuracy.

Fig. 1 shows a bifurcation diagram of the plate under analysis computed at $(\xi,\eta)=(0.0,0.0)$ and Fig. 2 shows similar diagrams at $(\xi,\eta)=(0.5,0.0)$. The pair $(\xi,\eta)$ are the non-dimensional coordinates $(x/a,y/b)$ and $W_i(\xi,\eta)$, $i=0$–3, represents the vibration amplitude of harmonic $i$ at $(\xi,\eta)$. Fig. 1 only shows the amplitudes of the first and third harmonics, because the other harmonics are zero at $(\xi,\eta)=(0.0,0.0)$.

In this text "main branch" designates a branch that contains a solution that simultaneously obeys the following: occurs at zero vibration amplitude, corresponding to a linear mode shape; occurs at a linear natural frequency or at a sub-harmonic of a linear natural frequency. A secondary branch is one that bifurcates from a main branch.

The continuation method was started at the first linear mode, very low amplitude and harmonic motion; a hardening spring effect followed accompanied by the appearance of the third harmonic (which can be seen in Figs. 1(b) and 2(d)). In this way, the first main branch represented by a thick black line was defined. A bifurcation point and a secondary branch were found after $\omega/\omega_{\ell1}=1.002$; these are due to a 1:3 internal resonance between modes (1,1) and (2,2) (number of half waves in the $x$ and $y$ directions, respectively), modes that can also be designated as modes number 1 and 4, if ordered according to growing linear natural frequencies. This secondary branch will be designated as symmetric secondary branch, because it only contains

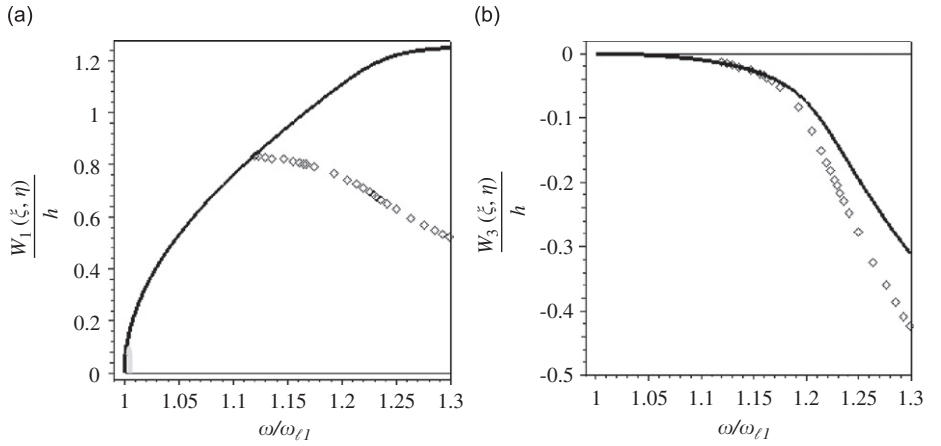


Fig. 1. Bifurcation diagrams computed at point $(\xi,\eta) = (0.0,\ 0.0)$; ▬ first main branch; — second main branch; ▬ symmetric secondary branch, ◇ asymmetric secondary branch: (a) first harmonic; (b) third harmonic.

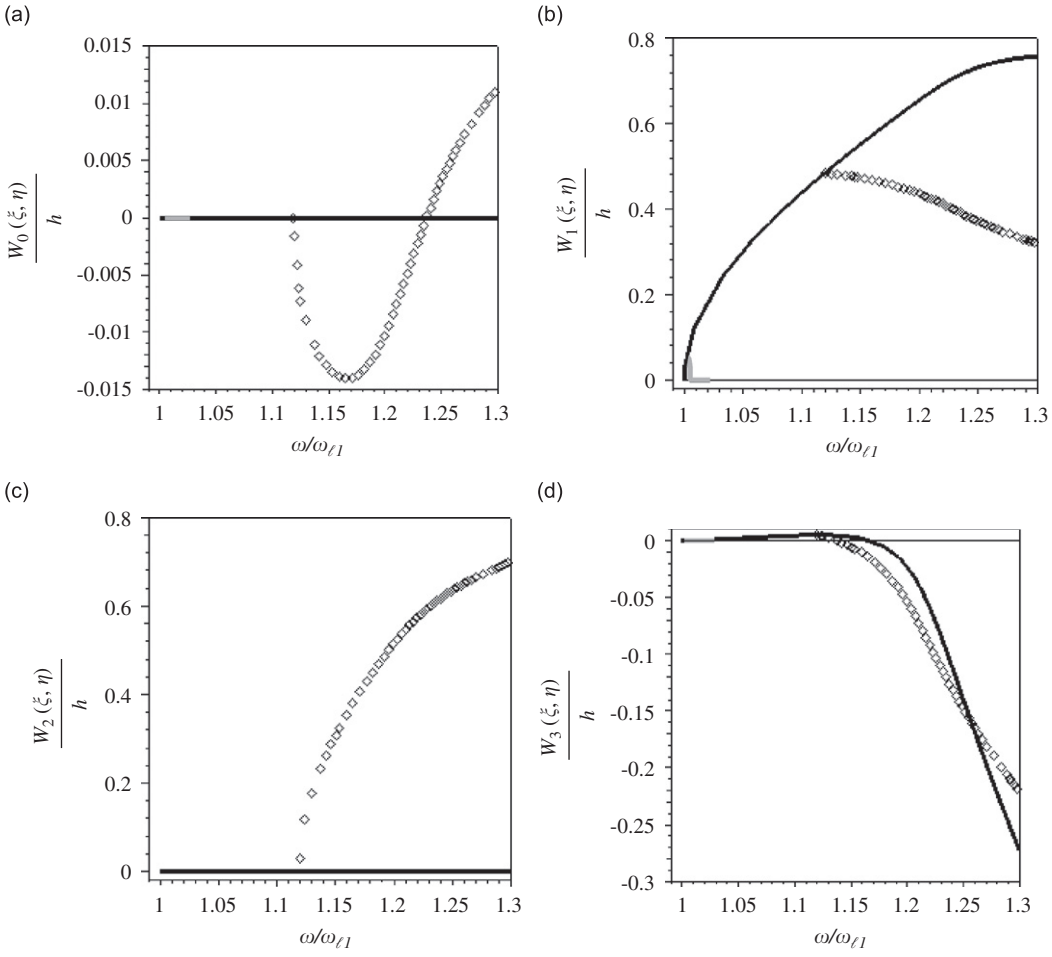


Fig. 2. Bifurcation diagrams computed at point $(\xi,\eta) = (0.5,\ 0.0)$; ▬ first main branch; — second main branch; ▬ symmetric secondary branch, ◇ asymmetric secondary branch: (a) first harmonic; (b) third harmonic; (c) second harmonic and (d) third harmonic.

solutions that have symmetry properties, revealed, for example, in the projection of trajectories on phase planes, which are symmetric with respect to the horizontal and vertical axis. The symmetric secondary branch leads to a second main branch, connected with mode (2, 2) and starting at $\omega_{\ell 4}/3$. The constant term and the second harmonic play no role whatsoever in the two main branches and in the symmetric secondary branch. On the contrary, the only reason why the amplitude of the third harmonic appears as zero on the second main branch is that Figs. 1 and 2 represent amplitudes on the nodal line of mode (2,2); the third harmonic is in fact present in the solutions. These data agree with the results computed in Ref. [1], where only odd harmonics were employed in the model.

At $\omega/\omega_{\ell 1} \cong 1.12$ ($\omega/\omega_{\ell 1}$ between 1.1188 and 1.1198) another bifurcation point occurs with the appearance of another secondary branch (which will be called asymmetric secondary branch because it contains asymmetric solutions). Figs. 1 and 2 show that all harmonics are different from zero in this branch and that the second harmonic steadily increases as the frequency increases. This bifurcation point and the asymmetric secondary branch were not found in Ref. [1] that treated exactly the same plate; moreover, branches of this type were not found in Refs. [2–11] where qualitatively similar problems were addressed.

The relation between the linear natural frequencies of mode (2,1) and mode (1,1) is 2.12. As the vibration amplitude grows in the first main branch, conditions for a 1:2 internal resonance between these two modes appear; therefore, mode (2,1) and the second harmonic are excited. The shapes (see Fig. 3) of each harmonic provide an additional demonstration that the secondary branch is due to a 1:2 internal resonance involving modes (1,1) and (2,1) (i.e., the first and third modes).

On the asymmetric secondary branch and close to the bifurcation point ($\omega/\omega_{\ell 1} \cong 1.12$), the most important harmonic is the first. Then, as energy is transferred to the second harmonic, the first harmonic looses some weight. A growth of the third harmonic is also observed. Hence, in a large number of solutions on the asymmetric secondary branch all harmonics have some importance. As an example, Fig. 3 shows the shape of the plate associated with each harmonic when $\omega/\omega_{\ell 1} \cong 1.25$ in the asymmetric secondary branch. The shape of the first harmonic, Fig. 3(b), is similar to the linear mode shape (1,1), i.e., the first mode shape. The shape

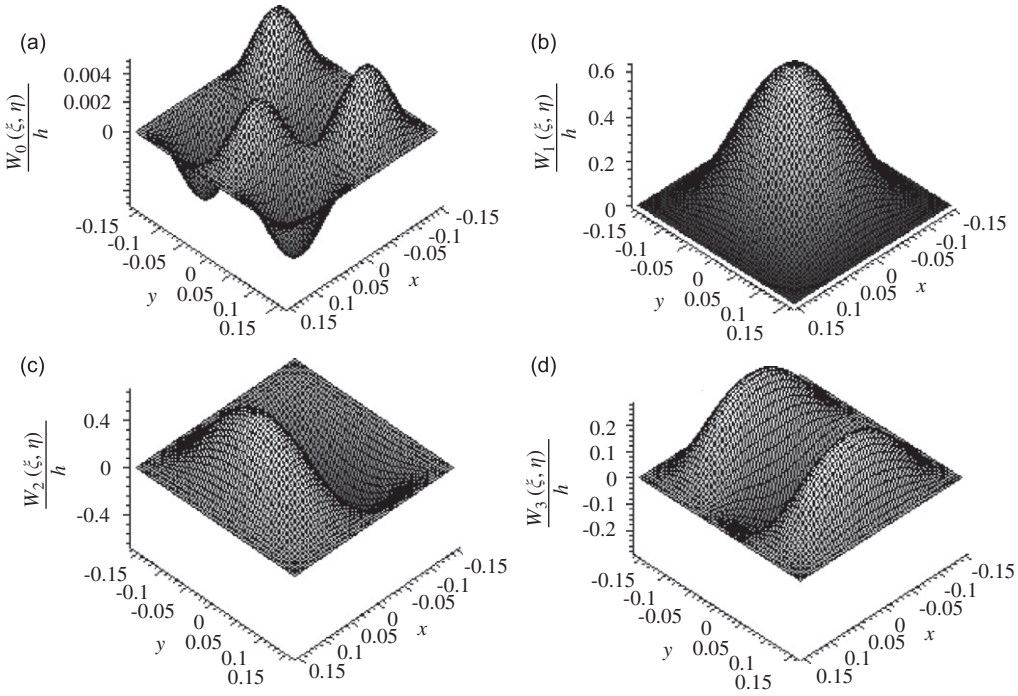


Fig. 3. Shapes of (a) constant term (divided by 2), (b) first, (c) second and (d) third harmonics at $\omega/\omega_{\ell 1} \cong 1.25$, asymmetric secondary branch.

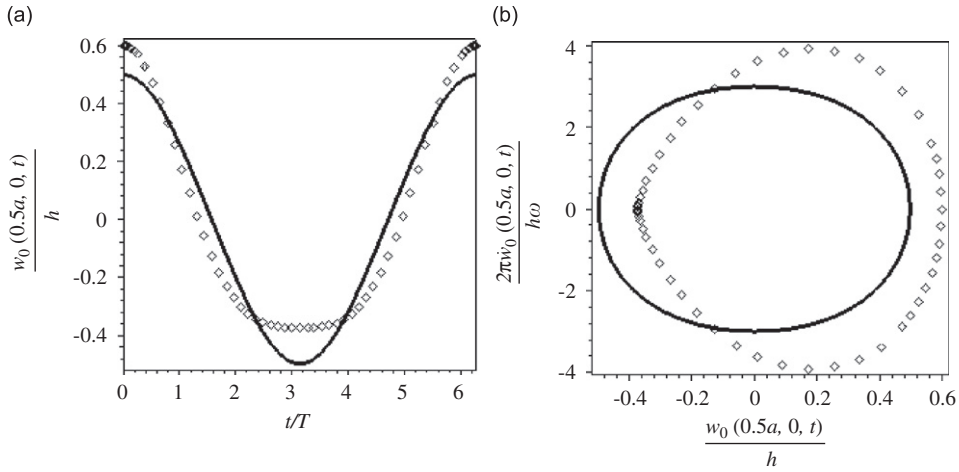


Fig. 4. Time history (a) and projection on a phase plane (b) of trajectories in first main branch (▬) and in the asymmetric secondary branch (◇), $\omega/\omega_{\ell 1} \cong 1.12$. Values at point ($x/a = 0.5$, $y/b = 0.0$).

of the second harmonic resembles that of the third linear mode shape (mode (2,1)), Fig. 3(c). In the third harmonic, the plate assumes a shape similar to the 5th linear mode shape (mode (1,3)).

Unlike what occurred in bifurcations due to 1:3 internal resonances between modes whose shapes have different types of symmetry (see paragraphs above and Refs. [1,6,11]), a connection between the asymmetric secondary branch due to a 1:2 internal resonance and a main branch beginning at the linear mode (2,1) was not found. This may have some relation with the increasing excitation of the third harmonic. Previous experiences with beams and plates indicate that modal interactions occurring between modes associated with shapes with similar symmetry properties do not lead to other branches Refs. [1,11]. Hence, we guess that the third harmonic is excited by an internal resonance between modes (1,3) and (1,1) that takes place on the asymmetric secondary branch. The relation between the linear natural frequencies of these modes is $\omega/\omega_{\ell 1} \cong 3.47$ and when the frequency of vibration increases conditions for 1:3 internal resonance are created.

Fig. 4 shows time histories and the projections of trajectories on a phase plane defined by the transverse displacement and velocity at point $x/a = 0.5$, $y/b = 0.0$. Two solutions that occur about $\omega/\omega_{\ell 1} \cong 1.12$ are shown, one is on the first main branch and the second is on the asymmetric secondary branch. Unlike the oscillation on the main branch, the oscillation on the asymmetric secondary branch occurs about a non-zero centre and the projection of the trajectory on the phase plane lost symmetry with respect to the vertical axis.

## 4. Conclusion

It was shown by means of an example that even harmonics can also appear in the geometrically nonlinear free vibrations of rectangular plates that are perfectly flat at rest. This demonstration is important because of three main reasons. First, the even harmonics are very often neglected in theoretical approaches, and therefore it is significant to demonstrate that they may appear, leading to qualitatively different solutions. Second, the conclusion that there are solutions where the even harmonics play no role confirms the (incomplete) results of a number of published analyses that neglected them from the start. Third, even harmonics were found in experimental analyses of beams and plates and the present study provides an alternative explanation for their appearance: bifurcations that lead the plate to vibrate about a non-flat equilibrium configuration. Naturally, there are other justifications for the appearance of even harmonics in experiments, including the facts that experimental specimens have imperfections and that the excitation system may itself introduce the even harmonics (see Refs. [19,20]).

## References


[1] P. Ribeiro, M. Petyt, Non-linear free vibration of isotropic plates with internal resonance, *International Journal of Non-linear Mechanics* 35 (2000) 263–278.

[2] K. Takahashi, A method of stability analysis for non-linear vibration of beams, *Journal of Sound and Vibration* 67 (1979) 43–54.

[3] Y.K. Cheung, S.L. Lau, Incremental time-space finite strip method for non-linear structural vibrations, *Earthquake Engineering and Structural Dynamics* 10 (1982) 239–253.

[4] R. Benamar, M.M.K. Bennouna, R.G. White, The effects of large vibration amplitudes on the mode shapes and natural frequencies of thin elastic structures. Part II: fully clamped rectangular isotropic plates, *Journal of Sound and Vibration* 164 (1993) 295–316.

[5] R. Benamar, M.M.K. Bennouna, R.G. White, The effects of large vibration amplitudes on the mode shapes and natural frequencies of thin elastic structures. Part III: fully clamped rectangular isotropic plates-measurements of the mode shape amplitude dependence and the spatial distribution of harmonic distortion, *Journal of Sound and Vibration* 175 (1994) 377–395.

[6] R. Lewandowski, Non-linear free vibrations of beams by the finite element and continuation methods, *Journal of Sound and Vibration* 170 (1994) 577–593.

[7] R. Lewandowski, Solutions with bifurcation points for free vibration of beams: an analytical approach, *Journal of Sound and Vibration* 177 (1994) 239–249.

[8] T.D. Burton, M.N. Hamdan, On the calculation of non-linear normal modes in continuous systems, *Journal of Sound and Vibration* 197 (1996) 117–130.

[9] R. Lewandowski, On beams membranes and plates vibration backbone curves in cases of internal resonance, *Meccanica* 31 (1996) 323–346.

[10] R. Lewandowski, Computational formulation for periodic vibration of geometrically nonlinear structures—Part 2: numerical strategy and examples, *International Journal Solids Structures* 34 (1997) 1949–1964.

[11] P. Ribeiro, M. Petyt, Non-linear vibration of beams with internal resonance by the hierarchical finite element method, *Journal of Sound and Vibration* 224 (1999) 591–624.

[12] M.M. Bennouna, R.G. White, The effects of large vibration amplitudes on the fundamental mode shape of a clamped–clamped uniform beam, *Journal of Sound and Vibration* 96 (1984) 309–331.

[13] M. Amabili, Theory and experiments for large-amplitude vibrations of rectangular plates with geometric imperfections, *Journal of Sound and Vibration* 291 (2006) 539–565.

[14] M. Amabili, *Nonlinear Vibrations and Stability of Shells and Plates*, Cambridge University Press, Cambridge, 2008.

[15] C.Y. Chia, *Nonlinear Analysis of Plates*, McGraw-Hill, New York, 1980.

[16] P. Ribeiro, On the influence of membrane inertia and shear deformation on the geometrically non-linear vibrations of open, cylindrical, laminated clamped shells, *Composites Science and Technology* 69 (2009) 176–185.

[17] P. Ribeiro, Non-linear free periodic vibrations of open cylindrical shallow shells, *Journal of Sound and Vibration* 313 (2008) 224–245.

[18] R. Lewandowski, Computational formulation for periodic vibration of geometrically nonlinear structures—Part 1: theoretical background, *International Journal of Solids and Structures* 34 (1997) 1925–1947.

[19] G.R. Tomlinson, Force distortion in resonance testing of structures with electro-dynamic vibration exciters, *Journal of Sound and Vibration* 63 (1979) 337–350.

[20] P. Ribeiro, The second harmonic and the validity of Duffing's equation for vibration of beams with large displacements, *Computers and Structures* 79 (2001) 107–117.